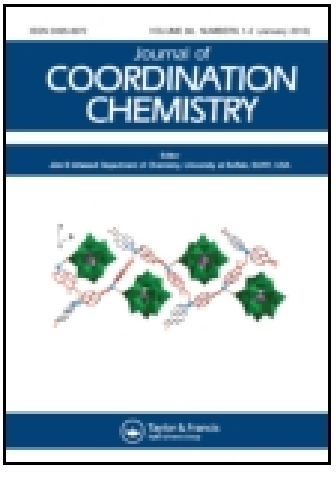

Journal of Coordination Chemistry
Publication details, including instructions for authors and subscription information:
http://www.tandfonline.com/loi/gcoo20

Three copper complexes containing the sulfur-bridged bis-pyridine ligands, 2,2′-dithiodipyridine and di-2-pyridyl sulfide

Mi Pan[a], Wei-Xia Zhou[a], Wang Yang Ma[a], Jiao Niu[a] & Jun Li[a]
[a] Key Laboratory of Synthetic and Natural Functional Molecule Chemistry of Ministry of Education, College of Chemistry and Materials Science, Northwest University, Xi'an, PR China
Accepted author version posted online: 01 Sep 2014.Published online: 23 Sep 2014.

To cite this article: Mi Pan, Wei-Xia Zhou, Wang Yang Ma, Jiao Niu & Jun Li (2014) Three copper complexes containing the sulfur-bridged bis-pyridine ligands, 2,2′-dithiodipyridine and di-2-pyridyl sulfide, Journal of Coordination Chemistry, 67:19, 3176-3187, DOI: 10.1080/00958972.2014.960860

To link to this article: http://dx.doi.org/10.1080/00958972.2014.960860

Journal of Coordination Chemistry, 2014
Vol. 67, No. 19, 3176–3187, http://dx.doi.org/10.1080/00958972.2014.960860

Three copper complexes containing the sulfur-bridged bis-pyridine ligands, 2,2′-dithiodipyridine and di-2-pyridyl sulfide

MI PAN, WEI-XIA ZHOU, WANG YANG MA, JIAO NIU and JUN LI*

Key Laboratory of Synthetic and Natural Functional Molecule Chemistry of Ministry of Education, College of Chemistry and Materials Science, Northwest University, Xi'an, PR China

(*Received 13 April 2013; accepted 24 July 2014*)

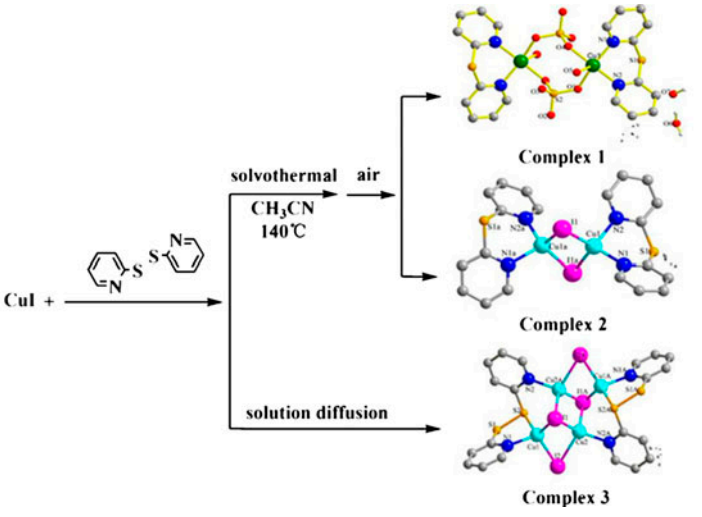

Three copper complexes constructed with sulfur-bridged bis-pyridine ligands 2,2′-dithiodipyridine (dtdp) and di-2-pyridyl sulfide (dps), $[Cu_2(dps)_2(H_2O)_2(\mu\text{-}SO_4)_2]\cdot(H_2O)_2$ (**1**), $[Cu_2I_2(dps)_2]$ (**2**), and $[Cu_4I_4(dtdp)_2]$ (**3**), have been synthesized by reaction of copper(I) iodide with dtdp under solvothermal and solution-diffusion conditions, and characterized by single crystal X-ray diffraction. The dps ligands were generated via *in situ* cleavage of S–S and S–C(py) bonds of dtdp. Cu ions are divalent in **1**, implying involvement of the starting Cu^+ cations in a redox process, while the Cu ions remained univalent in **2** and **3**. In **1** and **2**, the dps adopted N,N-chelate coordination, in contrast to the N,S-chelation of the dtdp ligand in **3**. Complex **1** displays a 2-D framework linked by hydrogen bonds and was further connected into a 3-D supramolecular structure by π–π stacking interactions between adjacent layers. Complexes **2** and **3** exhibited 2-D layer structures through π–π stacking interactions. The luminescent properties of **2** and **3** were also studied in the solid state at room temperature.

Keywords: Copper complex; 2,2′-Dithiodipyridine; Di-2-pyridyl sulfide; Crystal structure; Luminescent property

*Corresponding author. Email: junli@nwu.edu.cn

1. Introduction

There has been continuous interest in the coordination chemistry of copper complexes, and much attention has been paid to the design and synthesis of Cu(I) and Cu(II) complexes [1–5]. These complexes have been widely used in metal organic framework materials (MOFs), luminescent materials, magnetic materials, and efficient catalysts [6–9]. Complexes with bispyridine-type ligands incorporating other heteroatoms have been developed [10–13]. Pyridinethiones and their derivatives bearing both N and S donors offer opportunities for the construction of bi- and multidentate complexes [14–18].

To synthesize new copper coordination compounds with potential applications as MOFs or luminescent materials, and to find novel *in situ* ligand reactions, we used copper(I) iodide and a 2,2′-dithiodipyridine (dtdp) as reactants and obtained three new copper(I) and copper (II) complexes containing two kinds of sulfur-bridged bispyridine ligands, dtdp, and di-2-pyridyl sulfide (dps). In $[Cu_2(dps)_2(H_2O)_2(\mu\text{-}SO_4)_2]\cdot(H_2O)_2$ (**1**) and $[Cu_2I_2(dps)_2]$ (**2**), Cu^{2+} and Cu^{+} coordinate to nitrogen of dps. In $[Cu_4I_4(dtdp)_2]$ (**3**), there are two crystallographically independent Cu^{+} cations, one coordinates to N and S from a dtdp and two iodides, while the other is bound to a nitrogen from the ligand and three neighboring iodides. The luminescent properties of **3** were also studied in the solid state at room temperature.

2. Experimental

2.1. *Materials and methods*

All reagents were purchased from commercial sources and used without purification. C, H, and N microanalyses were performed on an Elemental Vario EL III elemental analyzer. UV–vis spectra were recorded on a Shimadzu UV-1800 UV–vis–NIR spectrophotometer. FT-IR spectra were obtained with samples in a KBr matrix on a ABEQUZNDX-550 series FT-IR spectrophotometer from 4000 to 400 cm^{-1}. ^1H NMR spectra were recorded at room temperature using a Varian Inova 400 MHz instrument and referenced to tetramethylsilane. Mass spectra (MS) were carried out on a microTOF-Q II mass spectrometer (Bruker). The solid-state luminescence spectrum was recorded at room temperature on a Hitachi F4500 fluorescence spectrofluorometer with a xenon arc lamp as the light source. Thermogravimetric analysis (TGA) of samples were performed under a N_2 atmosphere with a heating rate of 10 °C min^{-1} from room temperature to 1000 °C on a.

2.2. *Preparation of 1 and 2*

CuI (0.2 mM, 0.0381 g) and dtdp (0.10 mM, 0.0220 g) were dissolved in MeCN (8 mL). The solution was transferred to a 25-mL Teflon-lined steel autoclave, heated in an oven to 140 °C for 96 h, and then was gradually cooled to room temperature over 24 h. Some yellow microcrystals of **2** (as identified by PXRD, see figure S3, see online supplemental material at http://dx.doi.org/10.1080/00958972.2014.960860) were present, and the color of the solution was orange. After filtration, the filtrate solvent was allowed to evaporate at room temperature. Green column-shaped crystals of **1** (0.0133 g, 17% yield based on CuI) and yellow block-shaped crystals of **2** (0.0069 g, 9% yield based on CuI) were obtained after one week. Crystals of **1** and **2** were separated by hand according to their different colors and shapes.

For **1**: Elem. Anal. for $C_{20}H_{24}Cu_2N_4O_{12}S_4$. Calcd: C, 31.29; H, 3.15; N, 7.30. Found (%): C, 31.02; H, 3.35; N, 7.68. FTIR (KBr, cm^{-1}): 3447 ν(O–H), 2924 ν(C–H(py)), 1584 ν(C=N (py)), 1425 ν(C=C (py)), 1115 ν(C–S), 781 δ(C–H), 619 ν(Cu–N). MS (*m/z*, M + 1): 768.8 UV–vis (nm, CH_3CN): 286 ($\pi \rightarrow \pi^*$ transition of dps ligand), 358 (Cu^{2+} -dps charge transition).

For **2**: Elem. Anal. for $C_{20}H_{16}Cu_2I_2N_4S_2$. Calcd: C, 31.43; H, 2.11; N, 8.25. Found (%): C, 31.18; H, 2.37; N, 8.61. FTIR (KBr, cm^{-1}): 2924 ν(C–H(py)), 1578 ν(C=N (py)), 1416 ν(C=C (py)), 1115 ν(C–S), 760 δ(C–H). MS (*m/z*, M + 1): 758.8. UV–vis (nm, CH_3CN): 235 ($\pi \rightarrow \pi^*$ transition of dps ligand), 278 ($n \rightarrow \pi^*$ transition of dps ligand). ^1H NMR (400 MHz, $(CD_3)_2SO$): 8.49 (d, J = 3.9 Hz, 4H), 7.83–7.79 (m, 4H), 7.63 (d, J = 8.1 Hz, 4H), 7.29 (dd, J = 5.1 Hz, 4H).

2.3. *Preparation of 3*

An EtOH (6 mL) solution of dtdp (0.20 mM, 0.04406 g) was slowly layered onto a KI-saturated, aqueous solution of CuI (0.20 mM, 0.0381 g). The layered solutions were then kept at room temperature. After two weeks, yellow block-shaped crystals (0.0259 g, 43% yield based on CuI) were obtained after filtering and drying in air. Elem. Anal. for $C_{20}H_{16}Cu_4I_4N_4S_4$. Calcd: C, 19.98; H, 1.34; N, 4.66. Found (%): C, 19.72; H, 1.46; N, 4.83. IR (KBr, cm^{-1}): 2924 ν(C–H (py)), 1580 ν(C=N (py)), 1448 ν(C=C (py)), 1283 ν(C–C (py)), 1047 ν(C–S), 756 δ(C–H). MS (*m/z*, M + 1): 1203.4. UV–vis (nm, CH_3CN):

Table 1. Summary of the crystal, data collection, and refinement parameters for **1**–**3**.

Complexes	**1**	**2**	**3**
Empirical formula	$C_{20}H_{24}Cu_2N_4O_{12}S_4$	$C_{20}H_{16}Cu_2I_2N_4S_2$	$C_{20}H_{16}Cu_4I_4N_4S_4$
M (g M^{-1})	767.75	757.37	1202.37
Crystal system	Triclinic	Monoclinic	Orthorhombic
Space group	*P-1*	*C2/c*	*Pbca*
a (Å)	7.1868 (16)	15.820 (3)	10.505 (2)
b (Å)	9.425 (2)	12.167 (2)	14.377 (3)
c (Å)	11.660 (2)	14.264 (3)	19.957 (5)
α (°)	66.547 (3)	90	90
β (°)	80.580 (4)	101.328 (4)	90
γ (°)	81.707 (4)	90	90
V (Å^3)	712.1 (3)	2691.9 (9)	3014.1 (12)
Z	1	4	4
D_{Calcd} (g cm^{-3})	1.790	1.869	2.650
F (0 0 0)	390	1440	2224
μ (mm^{-1})	1.854	4.042	7.178
Independent reflections (R_{int})	3574	6727	13,811
Observed reflections [$I > 2r(I)$]	2476	2505	2675
Parameters refined	207	136	164
R_{int}	0.0221	0.0387	0.1598
R_1[a]/wR_2[b] [$I > 2r(I)$]	R_1 = 0.0424, wR_2 = 0.1094	R_1 = 0.0417, wR_2 = 0.1181	R_1 = 0.1145, wR_2 = 0.2095
R_1/wR_2 (all reflections)	R_1 = 0.0512, wR_2 = 0.1168	R_1 = 0.0647, wR_2 = 0.1302	R_1 = 0.1623, wR_2 = 0.2297
Goodness-of-fit[c] (GOF) on F^2	1.068	1.103	1.257
Largest diff. in peak/hole (e Å^{-3})	0.886/−0.409	0.757/−0.642	1.413/−1.312

[a]$R_1 = [\Sigma(||F_o|| - ||F_c||)/\Sigma|F_o|]$.
[b]$wR_2 = [\Sigma[w(F_o^2 - F_c^2)^2]]^{1/2}$.
[c]Goodness-of-fit $S = [\Sigma w(F_o^2 - F_c^2)^2/(n-p)]^{1/2}$, where n is the number of reflections and p the number of parameters.

234 ($\pi \rightarrow \pi^*$ transition of dtdp ligand), 276 ($n \rightarrow \pi^*$ transition of dtdp ligand). ^{1}H NMR (400 MHz, $(CD_3)_2SO$) δ 8.49 (s, 4H), 7.81 (t, J = 7.5 Hz, 4H), 7.63 (d, J = 7.9 Hz, 4H), 7.32–7.28 (m, 4H).

2.4. *X-ray crystal structure determinations*

Crystallographic data-sets were obtained at 296 K with a Bruker SMART CCD diffractometer with graphite-monochromated Mo Kα radiation (λ = 0.71073 Å). Absorption corrections were applied using SADABS [19]. The structures were solved by direct methods and refined by Fourier full-matrix least-squares calculations using anisotropic displacement parameters for all nonhydrogen atoms [20]. The hydrogens on carbon were placed in calculated positions with a fixed C–H distance (0.97 Å). Hydrogens on O in **1** were located from the difference maps and refined independently. Crystal, data collection, and refinement parameters are given in table 1.

3. Results and discussion

3.1. *Structure description*

3.1.1. Crystal structure of 1. Figure 1 illustrates the structure of **1**, and selected bond distances and angles are given in table 2. A characteristic feature of dtdp is the easy cleavage of the S–S bond. Hence, in the solvothermal reaction, dps was generated in part via *in situ* cleavage of the S–S bond of d*t*d*p*. The single-crystal X-ray structural analysis revealed that **1** crystallized in the triclinic space group *P-1*, and the asymmetric unit consists of one Cu, one dps, one coordinated SO_4^{2-}, one coordinated water, and two lattice waters. The Cu^{2+} cation exhibits a slightly distorted square pyramidal geometry [figure 1(a)] coordinated by two N (Cu(1)–N(1) = 1.998(3), Cu(1)–N(2) = 2.007(3) Å) from one dps, two O (Cu(1)–O(1) = 1.946(3), Cu(1)–O(4) = 1.946(3) Å) from SO_4^{2-}, and one water (Cu(1)–O(5) = 2.295(4) Å). The basal plane is formed by N1, N2, O1, and O4, and the Cu^{2+} is displaced from the mean basal plane toward the apically coordinated water by 0.098 Å. The sulfates symmetrically bridge two Cu^{2+} cations and form a chair-like eight-membered ring with a Cu···Cu distance of 4.913 Å.

The complex $[\mu\text{-(ox)}\{Cu(dps)(H_2O)\}_2](ClO_4)_2$ (ox = oxalate, $C_2O_4^{2-}$) [21] presents a similar structure, except that oxalate instead of sulfate is the bridging ligand. The Cu(II) center in this complex shows the same distorted square-pyramidal geometry as **1**, with basal Cu–O and Cu–N and apical Cu–O (water) distances equivalent to those observed in **1**. Another reported complex, $[Cu_2(HL^1)_2(\mu\text{-}SO_4)_2]\cdot 4H_2O$ (HL^1 = diacetyl monoxime-2-pyridyl hydrazone) [22], contains the same $\mu\text{-}SO_4^{2-}$ ligand, but the Cu^{2+} cation located in a more distorted square-pyramidal geometry, and the Cu···Cu distance (4.555 Å) is shorter than that in **1**.

The molecules of **1** are connected into a 2-D supramolecular network [figure 1(b)] along the *ac* plane through the hydrogen bonds O(5)–H(5B)…O(3) and O(5)–H(5A)···O(2)#1 (symmetry #1: $x - 1$, y, z) between SO_4^{2-} and coordinated water, and the hydrogen bonds O(6)–H(6A)…O(7), O(6)–H(6A)…O(7)#2, O(7)–H(7A)…O(6)#2, O(7)–H(7B)···O(3)#3, and O(7)–H(7B)…O(2)#3 (symmetry #2: $-x + 1$, $-y + 1$, $-z + 2$; #3: x, $y + 1$, z) between the SO_4^{2-} and lattice waters. The hydrogen bond distances and angles are given in table 3. Also, the 2-D supramolecular networks are further connected by π–π stacking interactions between the pyridine rings of adjacent dimers (3.679 Å) into a 3-D supramolecular structure, as shown in figure 1(c).

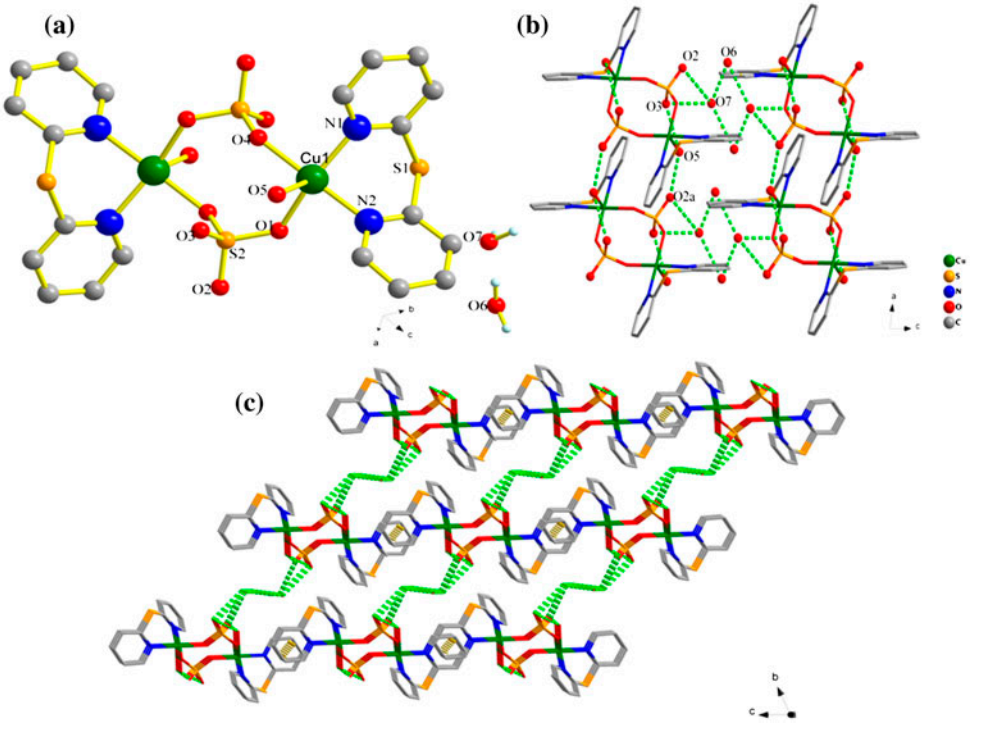

Figure 1. (a) View of **1** shown with 30% probability displacement ellipsoids; hydrogens were omitted for clarity. (b) View of the 2-D supramolecular network formed by hydrogen bonds between sulfate anions, coordinated water, and lattice water along the *ac* plane. Green dotted lines represent the hydrogen bonds; the hydrogens were omitted for clarity. (c) View of the 3-D supramolecular network formed by π–π stacking interactions between pyridine rings of the adjacent dimers along the *bc* plane (see http://dx.doi.org/10.1080/00958972.2014.960860 for color version).

3.1.2. Crystal structure of 2. Single-crystal X-ray analysis revealed that **2** has a dimeric structure, as shown in figure 2(a). This complex crystallized in the monoclinic space group *C2/c*, and the asymmetric unit contains one univalent Cu, one iodide, and one dps generated via the *in situ* cleavage of the S–S bond of the dtdp ligand in the presence of Cu^{+}. Cu(1) adopts a distorted tetrahedral geometry and is coordinated by two I^{-} and two nitrogens from a dps. The Cu(1)–N(1) and Cu(1)–N(2) bond lengths are 2.057(6) and 2.056(6) Å, respectively, while the Cu(1)–I(1) and Cu–I(1)#1 bond lengths are 2.6363(11) and 2.5878(12) Å, respectively (see table 2). The bond angles around Cu(1) range from 95.3(2)° to 116.76(4)° and are normal for a distorted tetrahedral geometry. The Cu···Cu distance in **2** (2.6679(18) Å) is slightly shorter than the sum of the van der Waals radii (2.80 Å) of two Cu(I) ions. Based on relevant references [23, 24], there might exist Cu···Cu interactions in **2**. In both **1** and **2**, N,N-chelate coordination is preferred, while the sulfurs from dps are not involved in coordination. As shown in figure 2(b), C–H···π (3.626 Å) and π···π (3.845 Å) stacking interactions between pyridine rings of adjacent molecules were observed. As a result, a 2-D layer structure was formed with cavities with maximum diameter of 9.253 Å when viewed through the *ab* plane [figure 2(c)].

Table 2. Selected bond lengths (Å) and angles (°) for **1**–**3**.

Complex **1**			
Bond lengths (Å)			
Cu(1)–O(1)	1.946(3)	Cu(1)–O(4)#	1.946(3)
Cu(1)–N(1)	1.998(3)	Cu(1)–N(2)	2.007(3)
Cu(1)–O(5)	2.295(4)		
Angles (°)			
O(1)–Cu(1)–O(4)#1	95.07(13)	O(1)–Cu(1)–N(1)	165.49(14)
O(4)#–Cu(1)–N(1)	89.82(14)	O(1)–Cu(1)–N(2)	86.39(13)
O(4)#–Cu(1)–N(2)	178.27(14)	N(1)–Cu(1)–N(2)	88.98(14)
O(1)–Cu(1)–O(5)	90.07(14)	O(4)#–Cu(1)–O(5)	85.51(14)
N(1)–Cu(1)–O(5)	103.95(14)	N(2)–Cu(1)–O(5)	93.57(15)
Complex **2**			
Bond lengths (Å)			
Cu(1)–N(2)	2.056(6)	Cu(1)–N(1)	2.057(6)
Cu(1)–I(1)#1	2.5878(12)	Cu(1)–I(1)	2.6363(11)
Cu(1)–Cu(1)#1	2.6679(18)		
Angles (°)			
N(2)–Cu(1)–N(1)	95.3(2)	N(2)–Cu(1)–I(1)#1	113.49(16)
N(1)–Cu(1)–I(1)#1	112.36(17)	N(2)–Cu(1)–I(1)	108.57(15)
N(1)–Cu(1)–I(1)	108.21(17)	I(1)#1–Cu(1)–I(1)	116.76(4)
N(2)–Cu(1)–Cu(1)#1	120.02(16)	N(1)–Cu(1)–Cu(1)#1	144.36(18)
I(1)–Cu(1)–Cu(1)#1	58.40(4)	Cu(1)–I(1)–Cu(1)#1	61.41(4)
Complex **3**			
Bond lengths (Å)			
Cu(1)–I(1)	2.569(3)	Cu(1)–S(2)	2.387(7)
Cu(1)–I(2)	2.569(3)	Cu(2)–I(2)	2.767(4)
Cu(1)–N(1)	2.019(17)	Cu(2)–I(1)#1	2.684(3)
Cu(2)–I(1)	2.689(3)	Cu(2)–N(2)#1	2.058(16)
Cu(2)–Cu(1)	2.668(4)		
Angles (°)			
Cu(1)–I(2)–Cu(2)	59.86(9)	Cu(1)–I(1)–Cu(2)#1	73.68(10)
Cu(1)–I(1)–Cu(2)	60.93(9)		
N(2)#1–Cu(2)–I(1)#1	105.6(5)	I(1)#1–Cu(2)–I(2)	107.27(11)
I(1)–Cu(2)–I(2)	104.28(11)	Cu(2)#1–I(1)–Cu2	65.95(11)
N(2)#1–Cu(2)–I(1)	119.0(5)	I(1)#1–Cu(2)–I(1)	114.05(11)
N(2)#|–Cu(2)–I(2)	105.9(5)	N(1)–Cu(1)–S(2)	89.2(6)
N(1)–Cu(1)–I(2)	106.4(5)	S(2)–Cu(1)–I(2)	108.28(18)
N(1)–Cu(1)–I(1)	114.1(5)	S(2)–Cu(1)–I(1)	121.66(19)
I(2)–Cu(1)–I(1)	113.92(12)		

Note: Symmetry transformations used to generate equivalent atoms: for **1**: # $-x+1, -y, -z+1$; for **2**: #1 $-x, y, -z+3/2$; for **3**: #1: $-x+1, -y, -z+1$.

Table 3. Hydrogen bond distances (Å) and angles (°) for **1**.

D–H…A	*d*(D–H)	*d*(H…A)	*d*(D…A)	∠(DHA)
O(5)–H(5A)…O(2)#1	0.856	1.879	2.734	169.92
O(5)–H(5B)…O(3)	0.857	2.246	2.904	133.62
O(6)–H(6A)…O(7)	0.877	1.655	2.472	153.80
O(6)–H(6A)…O(7)#2	0.877	2.502	2.968	113.95
O(7)–H(7A)…O(6)#2	0.878	2.123	2.968	161.16
O(7)–H(7B)…O(3)#3	0.766	2.513	3.000	123.10
O(7)–H(7B)…O(2)#3	0.766	2.610	3.353	164.17
O(7)–H(7B)…S(2)#3	0.766	2.920	3.618	152.62

Note: Symmetry transformations used to generate equivalent atoms: #1 $x-1, y, z$; #2 $-x+1, -y+1, -z+2$; #3 $x, y+1, z$.

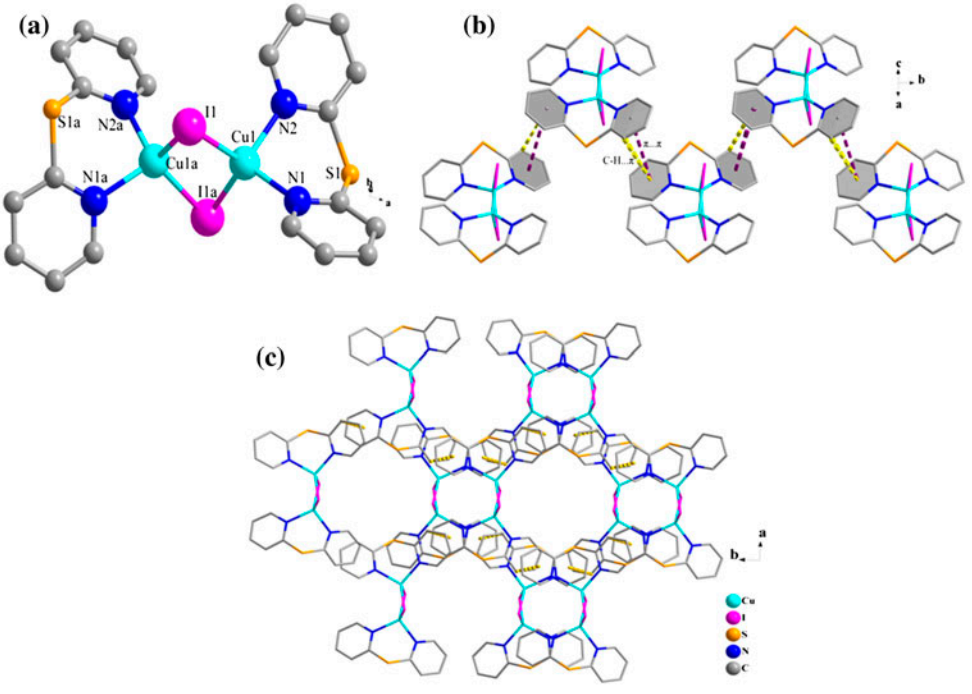

Figure 2. (a) View of **2** shown with 30% probability displacement ellipsoids; hydrogens were omitted for clarity. (b) View of the 2-D supramolecular networks formed by C–H…π interactions between the pyridine rings of adjacent dimers along the *ac* plane. (c) Same view along the *ab* plane.

Compared with literature reports, the Cu···Cu distance in **2** is slightly shorter than those of similar Cu(I) complexes containing pyridine and iodide, such as $Cu_2I_2L^2_4$ (L^2 = 3-methylpridine, 2.781(4) Å; pyridine, 2.698(2) Å; 3,5-dimethylpridine, 2.687(2) Å) [25–27], but longer than that in $Cu_2I_2(quin)_4$ (2.258(10) Å, quin = quinoline) [28]. The Cu–I and Cu–N bond lengths of **2** are normal relative to those of the previously mentioned [$Cu_2I_2L^2_4$] compounds [25–27].

3.1.3. Crystal structure of 3. As opposed to the solvothermal synthesis of **1** and **2**, tetramer **3** was formed at room temperature by layering of a dtdp solution over a CuI solution. Complex **3** crystallized in the orthorhombic space group *Pbca* with an asymmetric unit of two Cu(I) ions, two I^-, and one dtdp. As shown in figure 3(a), Cu(1) features a distorted tetrahedral geometry, coordinated to two I^- (Cu(1)–I(1) = 2.569(3), Cu(1)–I(2) = 2.569(3) Å) and one N (Cu(1)–N(1) = 2.019(17) Å) and one S (Cu(1)–S(2) = 2.387(7) Å) from one dtdp. Cu(2) also has a slightly distorted tetrahedral geometry constructed by three neighboring I^- (Cu(2)–I(1), 2.689(3) Å; Cu(2)–I(2), 2.767(4) Å; Cu(2)–I(1)#1, 2.684(3) Å) and one N (Cu(2)–N(2)#1 = 2.058(16) Å) from another dtdp. The Cu–I and Cu–N distances are comparable to those found in the distorted chair-like [$Cu_4I_4(L^3)_2$] structure (L^3 = 2-[(*o*-pyridyl)-sulfanylmethyl]pyridine, 2-[(*o*-pyridyl)-sulfanylmethyl pyrimidine]) [29, 30], and the Cu–S distance in **3** is at the high end of the range of Cu–S distances in tetrahedral Cu(I)

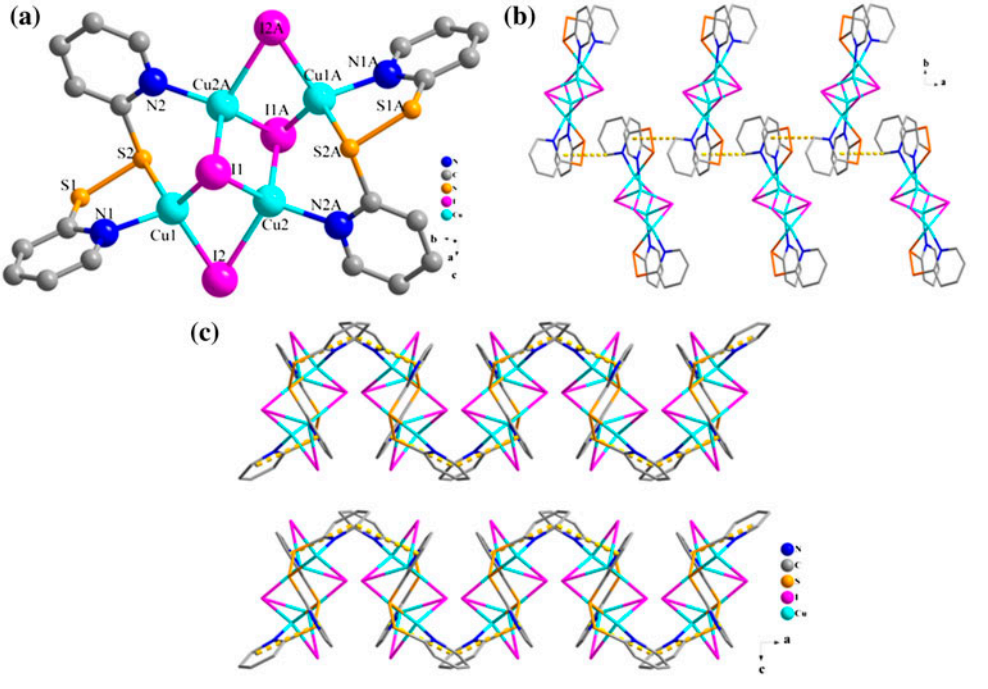

Figure 3. (a) View of **3** shown with 30% probability displacement ellipsoids; hydrogens were omitted for clarity. (b) View of the 2-D supramolecular network formed by edge-to-face π–π stacking interactions between the pyridine rings of adjacent units along the *ab* plane. (c) View of the 3-D stacking structure along the *ac* plane. Yellow dotted lines represent the π–π stacking interactions; hydrogens were omitted for clarity (see http://dx.doi.org/10.1080/00958972.2014.960860 for color version).

coordination complexes (2.303–2.382 Å) [31], but a little shorter than in $[Cu_4I_4(L^3)_2]$ (2.4158(12)–2.4395(14) Å) [29, 30].

The bond angles around Cu(1) range from 89.2(6)° to 121.66(19)°, and around Cu(2) they range from 104.28(11)° to 119.0(5)°. The tetrameric Cu_4I_4 core adopts a distorted chair-like structure. The dtdp behaves as a tridentate ligand with N(1) and S(2) chelating to Cu(1) while N(2) coordinates to Cu(2A). Complexes with similar N, S containing ligands 3-dpds and 4-dpds (3-dpds = di(3-pyridyl)disulfide, 4-dpds = di(4-pyridyl)disulfide) displayed only a Cu–N coordinating mode [32]. In addition, the short Cu···Cu distance (2.668 (4) Å) also indicates Cu···Cu interactions in **3**.

There are edge-to-face π–π stacking interactions between the pyridine rings of adjacent units (3.556 Å); thus **3** formed a 2-D layer supramolecular structure [figure 3(b)]. Figure 3(c) displays the zig–zag 3-D stacked structure along the *ac* plane.

3.2. *Plausible mechanism for formation of 1 and 2*

A similar *in situ* S–S bond cleavage reaction, that turned a disulfide into a thioether, has been reported [32–34]. Scheme 1 shows a plausible mechanism for the formation of **1** and **2**. Under solvothermal reaction conditions, the S–S and S–C(py) bonds of dtdp can undergo a Cu^+ cation-induced homolytic cleavage and form two free radicals (2-pyS·, 2-py·) and active [S] intermediates. The two free radicals can then recombine into dps. The *in situ* S–C bond

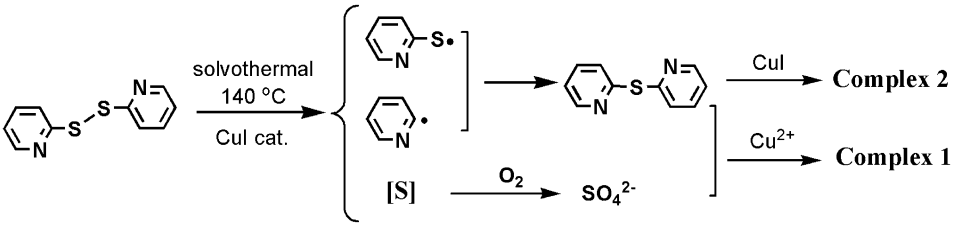

Scheme 1. A possible mechanism of the *in situ* ligand reaction for formation of **1** and **2**.

cleavage was also reported for pyridylmethylthioether, leading to formation of Cu(II) picolinate derivatives or oxorhenium(V) complexes of 2-(2-pyridylmethyl)ethane-1-thiol [35–37].

The active [S] intermediate can be oxidized by oxygen when the filtrate is exposed to air to produce SO_4^{2-}. The sulfate ion was identified by immediate formation of a white $BaSO_4$ precipitate when $BaCl_2$ was added to the cooled reaction solution. Thus, the newly formed dps ligand and SO_4^{2-} coordinate to a Cu(II) arising from oxidation of Cu(I), to form **1**, while only the dps coordinates to CuI to form **2**.

3.3. *Luminescence spectra of 2 and 3*

The solid-state emission spectra of **2** and **3** at room temperature are shown in figure 4. Upon excitation at 330 nm, two emission bands with peaks at 468 and 537 nm for **2**, and 468 and 521 nm for **3** were observed. The tetramer **3** showed stronger fluorescence emission than the dimer **2**. Similar to the photoluminescent properties of $(CuI)_n$ cluster complexes [38, 39], the emission band at 468 nm in the emission spectra of **2** and **3** may be assigned as a triplet halide to ligand charge transfer (^{3}XLCT) excited state, and the emission band at 537 nm (for **2**) and 521 nm (for **3**) to a combination of a triplet "cluster centered" (3CC*) excited state having mixed iodide to metal charge transfer and "metal cluster centered" d–s transitions [40, 41].

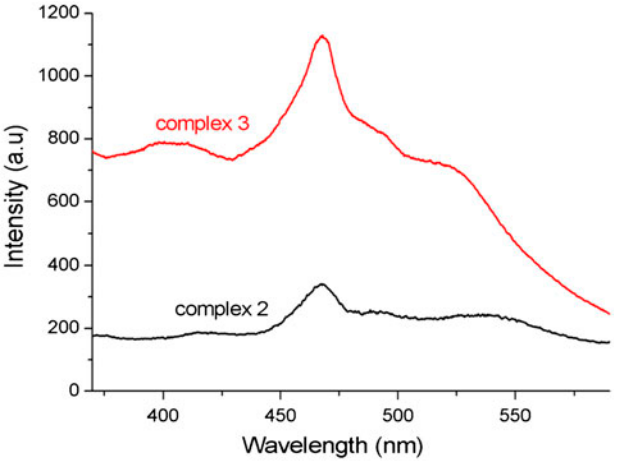

Figure 4. The emission spectra of **2** and **3** in the solid state at room temperature.

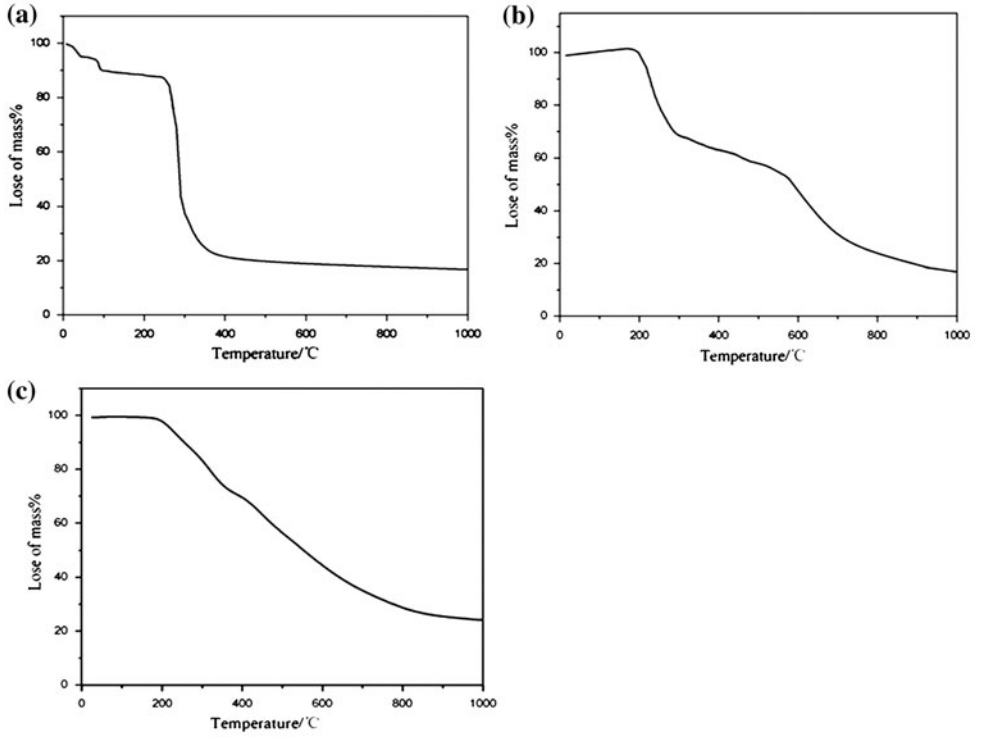

Figure 5. TG curves of **1** (a), **2** (b), and **3** (c).

3.4. *Thermogravimetric analysis*

The TGA curve of **1** [figure 5(a)] shows a three-step decomposition. The first and the second decomposition steps occur before 150 °C and correspond to sequential loss of two free waters and two coordinated waters (Found: 9.88 wt%, Calcd 9.38 wt%). Above 150 °C, **1** continues to decompose to the final residue of CuO (Found: 20.1 wt%, Calcd 20.7 wt%). For **2** [figure 5(b)], the first decomposition step between 180 and 610 °C corresponds to loss of two dps ligands (Found: 49.3 wt%, Calcd 49.7 wt%), the next step corresponds to loss of I_2 (Found: 33.6 wt%, Calcd 33.5 wt%), and the weight of the final residue is consistent with Cu (Found: 17.1 wt%, Calcd 16.8 wt%). The TGA curve of **3** [figure 5(c)] shows that it is stable to 190 °C and then decomposes gradually without any apparent plateau. The weight of the remaining residue is consistent with Cu (Found: 24.0 wt%, Calcd 21.2 wt%).

4. Conclusion

We report three copper complexes constructed by two kinds of sulfur-bridged bis-pyridine ligands, 2,2′-dithiodipyridine, and di-2-pyridyl sulfide. The di-2-pyridyl sulfide was generated via *in situ* cleavage of S–S and S–C(py) bonds of 2,2′-dithiodipyridine under the solvothermal synthesis conditions used for **1** and **2**. The copper ions adopted different coordination modes in the three complexes. Cu ions coordinated to both N and S in **3**,

in contrast to N,N′-coordination in **1** and **2**. Complex **1** displayed a 3-D supramolecular structure formed by hydrogen bonds and π–π stacking interactions. Complex **2** exhibited a 2-D layer structure through π–π stacking interactions. In **3**, the edge to face π–π stacking interactions between pyridine rings of adjacent units led to a 2-D layer supramolecular structure. The fluorescence spectra and thermal gravimetric analyses illustrate that **2** and **3** are fluorescent and possess thermal stability up to 180 °C.

Supplementary material

^{1}H NMR spectra for **2** and **3**; ESI-MS fragmentation patterns for **1–3**; PXRD pattern for the yellow microcrystals formed during the synthesis of **1** and **2**. CCDC 926478–926480 for **1–3** contain the supplementary crystallographic data. These data can be obtained free of charge via http://www.ccdc.cam.ac.uk/conts/retrieving.html or from the Cambridge Crystallographic Data Center, 12 Union Road, Cambridge CB2 1EZ, UK (Fax: +44 (0) 1223 336033; E-mail: deposit@ccdc.cam.ac.uk).

Funding

The authors acknowledge the research grant provided by the National Nature Science Foundation of China (Project No. 20971103 and 21271148) and the International Cooperation Project of Shaanxi province (2008KW-33) that resulted in this article.

References

[1] I. Castillo, V.M. Ugalde-Saldívar, L.A.R. Solano, B.N.S. Eguía, E. Zeglio, E. Nordlander. *Dalton Trans.*, **41**, 9394 (2012).
[2] E.V. Rybak-Akimova, A.Y. Nazarenko, L. Chen, P.W. Krieger, A.M. Herrera, V.V. Tarasov, P.D. Robinson. *Inorg. Chim. Acta*, **324**, 1 (2001).
[3] Z.L. You, D.M. Xian, M. Zhang. *CrystEngComm*, **14**, 7133 (2012).
[4] Y.-F. Liu, H.-T. Xia, D.-F. Rong. *J. Coord. Chem.*, **65**, 2919 (2012).
[5] A. Arnold, C. Limberg, R. Metzinger. *Inorg. Chem.*, **51**, 12210 (2012).
[6] S. Ferrer, E. Aznar, F. Lloret, A. Castiñeiras, M. Liu-González, J. Borrás. *Inorg. Chem.*, **46**, 372 (2007).
[7] M. Hashimoto, S. Igawa, M. Yashima, I. Kawata, M. Hoshino, M. Osawa. *J. Am. Chem. Soc.*, **133**, 10348 (2011).
[8] B.-L. Liu, J. Dang, S.-Q. Zang, Y.-X. Wang, R.-J. Tao. *Inorg. Chem. Commun.*, **14**, 31 (2011).
[9] O. Das, T.K. Paine. *Dalton Trans.*, **41**, 11476 (2012).
[10] J. Wang, Y.H. Zhang, H.X. Li, Z.J. Lin, M.L. Tong. *Cryst. Growth Des.*, **7**, 2352 (2007).
[11] F.M. Tabellion, S.R. Seidel, A.M. Arif, P.J. Stang. *J. Am. Chem. Soc.*, **123**, 7740 (2001).
[12] W.C. Silva, J.B. Lima, I.S. Moreira, A.M. Neto, F.C.G. Gandra, A.G. Ferreira, B.R. McGarvey, D.W. Franco. *Inorg Chem.*, **42**, 6898 (2003).
[13] J. Wang, S.L. Zheng, S. Hu, Y.H. Zhang, M.L. Tong. *Inorg. Chem.*, **46**, 795 (2007).
[14] R. Horikoshi, T. Mochida. *Coord. Chem. Rev.*, **250**, 2595 (2006).
[15] K. Sukcharoenphon, D. Moran, P.R. Schleyer, J.E. McDonough, K.A. Abboud, C.D. Hoff. *Inorg. Chem.*, **42**, 8494 (2003).
[16] F.M. Tabellion, S.R. Seidel, A.M. Arif, P.J. Stang. *J. Am. Chem. Soc.*, **123**, 7740 (2001).
[17] W.M. Teles, M.V. Marinho, M.I. Yoshida, N.L. Speziali, K. Krambrock, C.B. Pinheiro, N.M. Pinhal, A.A. Leitão, F.C. Machado. *Inorg. Chim. Acta*, **359**, 4613 (2006).
[18] O.S. Jung, Y.J. Kim, Y.A. Lee, H.K. Chae, H.G. Jang, J. Hong. *Inorg. Chem.*, **40**, 2105 (2001).
[19] G.M. Sheldrick. *SADABS, Program for Area Detector Adsorption Correction*, Institute for Inorganic Chemistry, University of Gottingen, Germany (1996).
[20] G.M. Sheldrick. *SHELX-97, Program for the Solution of Crystal Structures*, University of Göttingen, Germany (1997).
[21] D.M. de Faria, M.I. Yoshida, C.B. Pinheiro, K.J. Guedes, K. Krambrock, R. Diniz, L.F.C. de Oliveira, F.C. Machado. *Polyhedron*, **26**, 4525 (2007).

[22] C. Basu, S. Biswas, A.P. Chattopadhyay, H. Stoeckli-Evans, S. Mukherjee. *Eur. J. Inorg. Chem.*, **31**, 4927 (2008).
[23] J.K. Cheng, Y.G. Yao, J. Zhang, Z.J. Li, Z.W. Cai, X.Y. Zhang, Z.N. Chen, Y.B. Chen, Y. Kang, Y.Y. Qin, Y.H. Wen. *J. Am. Chem. Soc.*, **126**, 7796 (2004).
[24] M. O'Keeffe, N.E. Brese. *J. Am. Chem. Soc.*, **113**, 3226 (1991).
[25] N.P. Rath, J.L. Maxwell, E.M. Holt. *J. Chem. Soc., Dalton Trans.*, 2449 (1986).
[26] J.C. Dyason, L.M. Engelhardt, P.C. Healy, A.H. White. *Aust. J. Chem.*, **37**, 2201 (1984).
[27] P.C. Healy, C. Pakawatchai, A.H. White. *J. Chem. Soc., Dalton Trans.*, 1917 (1983).
[28] N.P. Rath, E.M. Holt, K. Tanimura. *J. Chem. Soc., Dalton Trans.*, 2303 (1986).
[29] Y.B. Xie, Z.C. Ma, D. Wang. *J. Mol. Struct.*, **784**, 93 (2006).
[30] Z.C. Ma, H.S. Xian. *J. Chem. Crystallogr.*, **36**, 129 (2006).
[31] E.S. Raper. *Coord. Chem. Rev.*, **91**, 129 (1994).
[32] M.M. Kadooka, L.G. Warner, K. Seff. *J. Am. Chem. Soc.*, **98**, 7569 (1976).
[33] T.S. Lobana, R. Sultana, G. Hundal, R.J. Butcher. *Dalton Trans.*, **39**, 7870 (2010).
[34] J. Wang, Y.H. Zhang, H.X. Li, Z.J. Lin, M.L. Tong. *Cryst. Growth Des.*, **7**, 2352 (2007).
[35] S. Sarkar, S. Dey, T. Mukherjee, E. Zangrando, M.G.B. Drew, P. Chattopadhyay. *J. Mol. Struct.*, **980**, 94 (2010).
[36] S. Sarkar, T. Mukherjee, S. Sen, E. Zangrando, P. Chattopadhyay. *J. Mol. Struct.*, **980**, 117 (2010).
[37] B. Das, S. Sarkar, E. Zangrando, P. Chattopadhyay. *Inorg. Chem. Commun.*, **12**, 1112 (2009).
[38] D.-P. Jiang, R.-X. Yao, F. Ji, X.-M. Zhang. *Eur. J. Inorg. Chem.*, **4**, 556 (2013).
[39] W.J. Gee, S.R. Batten. *Cryst. Growth Des.*, **13**, 2335 (2013).
[40] P.C. Ford, E. Cariati, J. Bourassa. *Chem. Rev.*, **99**, 3625 (1999).
[41] M. Vitale, P.C. Ford. *Coord. Chem. Rev.*, **219–221**, 3 (2001).